

Optical Engineering

OpticalEngineering.SPIEDigitalLibrary.org

Diffusion-based cooperative space object tracking

Bin Jia
Khanh Pham
Erik Blasch
Genshe Chen
Dan Shen

Diffusion-based cooperative space object tracking

Bin Jia,^{a,*} Khanh Pham,^b Erik Blasch,^c Genshe Chen,^a and Dan Shen^a

^aIntelligent Fusion Technology, Inc., Germantown, Maryland, United States

^bAir Force Research Lab, Kirtland Air Force Base, Albuquerque, New Mexico, United States

^cAir Force Office of Scientific Research, Arlington, Virginia, United States

Abstract. We propose the diffusion-based enhanced covariance intersection cooperative space object tracking (DeCiSpOT) filter. The main advantage of the proposed DeCiSpOT algorithm is that it can balance the computational complexity and communication requirements between different sensors as well as improve track accuracy when measurements do not exist or are of low accuracy. Instead of using the standard covariance intersection in the diffusion step, the enhanced diffusion strategy integrates the 0-1 weighting covariance intersection strategy and the iterative covariance intersection strategy. The proposed DeCiSpOT algorithm also uses the global nearest neighbor and probabilistic data association for multiple space object tracking. Two typical scenarios including cooperative single and multiple space object tracking are used to demonstrate the performance of the proposed DeCiSpOT filter. Using simulated ground-based electro-optical (EO) measurements for multiple resident space objects and multiple distributed EO sensors, the DeCiSpOT archived results comparable to an optimal centralized approach. The results demonstrate that the DeCiSpOT is effective for space object tracking problem with results close to the optimal centralized cubature Kalman filter. © 2019 Society of Photo-Optical Instrumentation Engineers (SPIE) [DOI: 10.1117/1.OE.58.4.041607]

Keywords: distributed tracking; space object; covariance intersection; Kalman filter; diffusion.

Paper 181315SS received Sep. 12, 2018; accepted for publication Dec. 18, 2018; published online Jan. 21, 2019.

1 Introduction

Multiple ground and space sensors are currently dedicated to achieving space situational awareness (SSA) due to the vast horizons and limited sensing field of view.¹ Traditionally, multiple sensors with limited bandwidth and power were not designed to cooperatively track space objects. With the advent of advanced sensor designs, deployment of more sensors, and increased communications capabilities, cooperative space object tracking (SpOT) is possible. Cooperative SpOT can be used for long-term or time-sensitive high-value SpOT and fast space event detection. SpOT and SSA²⁻⁴ are important to many space missions, such as global navigation, wireless communications, and distributed multimedia; which has received considerable attention in recent years. However, most of the work on SpOT focuses on single-sensor-single-object tracking. In this paper, multiple sensor-based space object tracking is developed for decentralized information cooperation. Due to the well-known advantages of decentralized processing (e.g., robustness, simplicity, and efficiency), distributed space object tracking using multiple sensors is preferred. Distributed cooperative tracking has been intensively researched and there are many strategies, such as gossip,⁵ consensus,⁶ and diffusion.⁷ Recently, the consensus-based SpOT has been proposed to use the information from multiple sensors.⁴ Specifically, the information weighted consensus strategy⁸ is used due to its simplicity to implement and its high accuracy. One practical issue for the diffusion-based cooperative SpOT algorithm is that the communication resources in the sensor network are limited. Hence, a communication efficient, cooperative SpOT algorithm is desired. In general, consensus-based algorithms require a large number of iterations to achieve agreement. In addition, there are many sensors within the network

that might not have observations (naïve nodes) for SSA due to various constraints. Hence, we propose using the enhanced diffusion strategy for the distributed space object tracking which considers the existence of naïve nodes and communications constraints for SSA.

This paper details diffusion-based SpOT using multiple sensors for scenarios with single and multiple space objects. The primary goal is maintaining existing tracks, where track initialization^{9,10} and termination are not considered in this paper. To associate the measurement and track, the global nearest neighbor (GNN) and joint probabilistic data association (JPDA)¹¹ algorithms are employed. Due to the essential nonlinearity of the space object tracking problem, nonlinear filters such as the unscented Kalman filter,¹² cubature Kalman filter (CKF),^{13,14} and sparse-grid quadrature filter^{15,16} are considered, where the cubature information filter (CIF) is demonstrated in this paper.

The remainder of the paper is organized as follows. The space object tracking problem using ground electro-optical (EO) sensors is introduced in Sec. 2. Section 3 introduces the centralized multiple sensor estimation for space object tracking. Section 4 describes a decentralized approach using the proposed diffusion-based SpOT algorithm. Two multiple sensor-based space object tracking scenarios are provided in Sec. 5 to illustrate the improved performance of the proposed algorithm. Section 6 gives the concluding remarks.

2 Background of Space Object Tracking

SpOT is considered in this paper using only ground EO sensors; however, the methods could be utilized by any SSA system using space object detections from different sensor types located on the ground or in space. This section reviews

*Address all correspondence to Bin Jia, E-mail: bin.jia@intfusiontech.com

the space object motion equation and an EO sensor measurement equation and the system constraints.

2.1 Dynamic Object Motion Equation

The dynamic equation of a near-earth space object is given by Refs. 17 and 18

$$\ddot{\mathbf{r}} = -\frac{\mu}{r^3}\mathbf{r} + \mathbf{a}_{J_2} + \mathbf{v}, \quad (1)$$

where $\mathbf{r} = [x, y, z]^T$ is the position of the space object in the inertial coordinate frame (I-J-K), μ is the standard gravitational constant, the range is $r = \sqrt{x^2 + y^2 + z^2}$, \mathbf{v} is the white Gaussian process noise, and \mathbf{a}_{J_2} corresponds to the J_2 perturbations

$$\mathbf{a}_{J_2} = -\frac{3}{2}J_2\left(\frac{R_E}{r}\right)^2 \cdot \frac{\mu}{r^3} \cdot \left[x\left(1 - 5\frac{z^2}{r^2}\right), y\left(1 - 5\frac{z^2}{r^2}\right), z\left(3 - 5\frac{z^2}{r^2}\right) \right]^T, \quad (2)$$

where R_E is the radius of the Earth and J_2 is the constant.

Note that in this paper, Eq. (1) does not consider drag and solar radiation pressure for simplicity. But these parameters can be incorporated when the mass and surface area of the space object are given.

2.2 EO Sensor Measurement Equation

The ground EO sensor measurement is described as

$$\begin{cases} az = \tan^{-1}(\rho_e/\rho_n) + n_{az} \\ el = \tan^{-1}\left(\rho_u/\sqrt{\rho_e^2 + \rho_n^2}\right) + n_{el} \end{cases}, \quad (3)$$

where the azimuth (az), the elevation (el), and the range $\boldsymbol{\rho} = [\rho_u, \rho_e, \rho_n]^T$ can be measured by the optical sensor on the ground with respect to the local observer coordinate system, ($\hat{\mathbf{u}} - \hat{\mathbf{e}} - \hat{\mathbf{n}}$; “up, east, and north”). Note that the covariance of measurement noise is assumed to be $\text{diag}([1 \text{ arc sec}, 1 \text{ arc sec}]^2)$.

The geometry of the observation model is shown in Fig. 1. The range can be related to the position vector in the inertial frame (I-J-K) by the coordinate transformation given as

$$\begin{bmatrix} \rho_u \\ \rho_e \\ \rho_n \end{bmatrix} = \begin{bmatrix} \cos \lambda & 0 & \sin \lambda \\ 0 & 1 & 0 \\ -\sin \lambda & 0 & \cos \lambda \end{bmatrix} \begin{bmatrix} \cos \theta & \sin \theta & 0 \\ -\sin \theta & \cos \theta & 0 \\ 0 & 0 & 1 \end{bmatrix} \times \begin{bmatrix} x - \|\mathbf{R}\| \cos \lambda \cos \theta \\ y - \|\mathbf{R}\| \cos \lambda \sin \theta \\ z - \|\mathbf{R}\| \sin \lambda \end{bmatrix}, \quad (4)$$

where $\|\mathbf{R}\| = 6378.1363 \text{ km}$ is the Earth radius; λ and θ are the latitude and local sidereal time of the observer, respectively; and n_{az} and n_{el} are white Gaussian measurement noise.

Measurements from the i 'th EO sensor will be unavailable when the line-of-sight path between the sensor and the space object is blocked by the Earth. The condition of

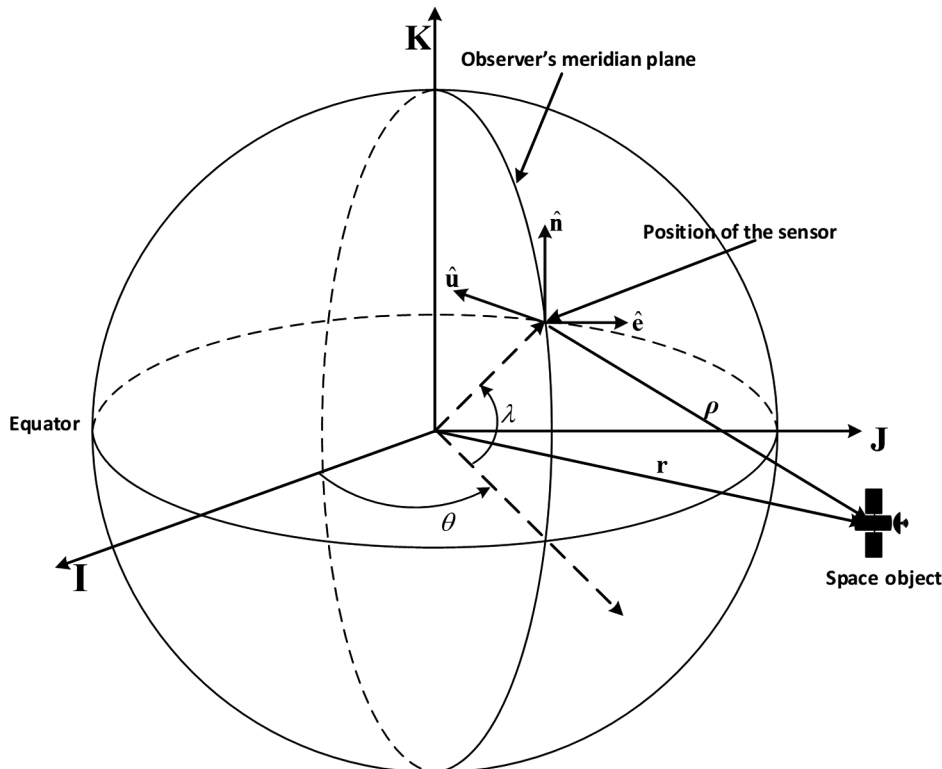


Fig. 1 Illustration of the observing geometry.

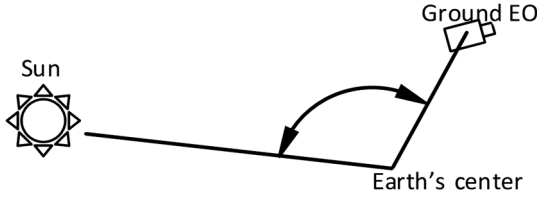


Fig. 2 Illustration of the dark background check.

the Earth blockage is examined between the distance function D and the radius of the Earth $R_E = \|\mathbf{R}\|$.¹⁸ If there exists $\vartheta \in [0,1]$ such that $D_{\vartheta}(i) < R_E$, where

$$D_{\vartheta}(i) = \sqrt{[(1-\vartheta)x_i + \vartheta x]^2 + [(1-\vartheta)y_i + \vartheta y]^2 + [(1-\vartheta)z_i + \vartheta z]^2}, \quad (5)$$

then the measurement from the i 'th sensor to the space object will be unavailable. The minimum of $D_{\vartheta}(i)$ is achieved at $\vartheta = \vartheta^*$, where ϑ^* is given as

$$\vartheta^* = -\frac{x_i(x-x_i) + y_i(y-y_i) + z_i(z-z_i)}{(x-x_i)^2 + (y-y_i)^2 + (z-z_i)^2}. \quad (6)$$

Thus, the system first examines whether $\vartheta^* \in [0,1]$ and then checks the Earth blockage condition $D_{\vartheta^*}(i) < R_E$.

Another geometric constraint for the EO sensor is that the dark background (night) is required. To satisfy a dark background, the angle (as shown in Fig. 2) between the vector from the Earth's center to the sensor and the vector from the Earth's center to the Sun should be greater than 102 deg.¹⁹

With the sensor measurements and geometrical checks, a cooperative tracking method can be coordinated using distributed sensors. To demonstrate the advantages of the decentralized space object tracking approach, a cooperative centralized information filter approach is first presented.

3 Centralized Cooperative Space Object Tracking

SpOT can be achieved for single and multiple objects.

3.1 Single Space Object Tracking

Consider a class of nonlinear discrete-time dynamical systems

$$\mathbf{x}_k = \mathbf{f}(\mathbf{x}_{k-1}) + \mathbf{v}_{k-1}, \quad (7)$$

$$\mathbf{z}_{k,j} = \mathbf{h}_j(\mathbf{x}_k) + \mathbf{n}_{k,j}, \quad (8)$$

where $\mathbf{x}_k \in \mathbf{R}^n$; $\mathbf{z}_{k,j} \in \mathbf{R}^m$. \mathbf{v}_{k-1} and $\mathbf{n}_{k,j}$ are independent white Gaussian process noise and measurement noise with covariance \mathbf{Q}_{k-1} and $\mathbf{R}_{k,j}$, respectively. $\mathbf{z}_{k,j}$ is the measurement by the j 'th sensor, $j = 1, \dots, N_{sn}$ and N_{sn} is the number of sensors.

For centralized fusion methods, the information filter is commonly used due to its simplicity and robustness for multiple sensor applications.²⁰ For the information filter, the information state and the information matrix at the time $k-1$ are defined by $\hat{\mathbf{y}}_{k-1|k-1} = \mathbf{P}_{k-1|k-1}^{-1} \hat{\mathbf{x}}_{k-1|k-1}$ and $\mathbf{Y}_{k-1|k-1} = \mathbf{P}_{k-1|k-1}^{-1}$, respectively. The system state $\hat{\mathbf{x}}_{k-1|k-1}$

and covariance $\mathbf{P}_{k-1|k-1}$ can be obtained by $\hat{\mathbf{x}}_{k-1|k-1} = \mathbf{P}_{k-1|k-1} \hat{\mathbf{y}}_{k-1|k-1}$ and $\mathbf{P}_{k-1|k-1} = \mathbf{Y}_{k-1|k-1}^{-1}$, respectively. In this paper, the CIF is used and it contains the prediction and update steps.

3.1.1 Cubature information filter predict step

The information state $\hat{\mathbf{y}}_{k|k-1}$ and the information matrix $\mathbf{Y}_{k|k-1}$ can be predicted as

$$\hat{\mathbf{y}}_{k|k-1} = \mathbf{P}_{k|k-1}^{-1} \hat{\mathbf{x}}_{k|k-1}, \quad (9)$$

$$\mathbf{Y}_{k|k-1} = \mathbf{P}_{k|k-1}^{-1}. \quad (10)$$

The predicted state and the associated covariance matrix at time k can be obtained as

$$\hat{\mathbf{x}}_{k|k-1} = \sum_{i=1}^{2n} W_i \mathbf{f}(\xi_{k,i}), \quad (11)$$

$$\mathbf{P}_{k|k-1} = \sum_{i=1}^{2n} W_i [\mathbf{f}(\xi_{k,i}) - \hat{\mathbf{x}}_{k|k-1}] [\mathbf{f}(\xi_{k,i}) - \hat{\mathbf{x}}_{k|k-1}]^T + \mathbf{Q}_k, \quad (12)$$

where $\xi_{k,i}$ is the transformed points from the covariance decomposition

$$\mathbf{P}_{k-1|k-1} = \tilde{\mathbf{S}}_{k-1|k-1} \tilde{\mathbf{S}}_{k-1|k-1}^T, \quad (13)$$

$$\xi_{k,i} = \tilde{\mathbf{S}}_{k-1|k-1} \boldsymbol{\gamma}_i + \hat{\mathbf{x}}_{k-1|k-1}, \quad (14)$$

where W_i and $\boldsymbol{\gamma}_i$ can be obtained via the cubature rule with

$$W_i = 1/(2n) \quad i = 1, \dots, 2n, \quad (15)$$

$$\boldsymbol{\gamma}_i = \begin{cases} \sqrt{n} \mathbf{e}_i & i = 1, \dots, n \\ -\sqrt{n} \mathbf{e}_{i-n} & i = n+1, \dots, 2n \end{cases}, \quad (16)$$

and \mathbf{e}_i is the unit vector in \mathbf{R}^n with the i 'th element being 1.

3.1.2 Cubature information filter update step

For multiple sensor estimation, the information state and the information matrix can be updated by Refs. 20 and 21

$$\hat{\mathbf{y}}_{k|k} = \hat{\mathbf{y}}_{k|k-1} + \sum_{j=1}^{N_{sn}} \mathbf{i}_{k,j}, \quad (17)$$

$$\mathbf{Y}_{k|k} = \mathbf{Y}_{k|k-1} + \sum_{j=1}^{N_{sn}} \mathbf{I}_{k,j}, \quad (18)$$

where the information state contribution $\mathbf{i}_{k,j}$ and the information matrix contribution $\mathbf{I}_{k,j}$ of the j 'th sensor are given by Ref. 21

$$\mathbf{i}_{k,j} = (\mathbf{P}_{k|k-1})^{-1} \mathbf{P}_{k|k-1, xz_j} \mathbf{R}_{k,j}^{-1} \{(\mathbf{z}_{k,j} - \hat{\mathbf{z}}_{k,j}) + (\mathbf{P}_{k|k-1, xz_j})^T [(\mathbf{P}_{k|k-1})^{-1}]^T \hat{\mathbf{x}}_{k|k-1}\}, \quad (19)$$

$$\mathbf{I}_{k,j} = (\mathbf{P}_{k|k-1})^{-1} \mathbf{P}_{k|k-1,xz_j} \mathbf{R}_{k,j}^{-1} (\mathbf{P}_{k|k-1,xz_j})^T [(\mathbf{P}_{k|k-1})^{-1}]^T, \quad (20)$$

where $\mathbf{R}_{k,j}$ is the covariance of the measurement noise corresponding to the j 'th measurement equation and

$$\hat{\mathbf{z}}_{k,j} = \sum_{i=1}^{2n} W_i h_j(\zeta_{k,i}), \quad (21)$$

$$\mathbf{P}_{k|k-1,xz_j} = \sum_{i=1}^{2n} W_i (\zeta_{k,i} - \hat{\mathbf{x}}_{k|k-1}) [h_j(\zeta_{k,i}) - \hat{\mathbf{z}}_{k,j}]. \quad (22)$$

Note that $\zeta_{k,i}$ are the transformed points obtained from the covariance decomposition:

$$\mathbf{P}_{k|k-1} = \tilde{\mathbf{S}}_{k|k-1} \tilde{\mathbf{S}}_{k|k-1}^T, \quad (23)$$

$$\zeta_{k,i} = \tilde{\mathbf{S}}_{k|k-1} \boldsymbol{\gamma}_i + \hat{\mathbf{x}}_{k|k-1}. \quad (24)$$

Remark 3.1: From the above cubature information filter algorithm, it can be seen that the local information contributions of $\mathbf{i}_{k,j}$ and $\mathbf{I}_{k,j}$ are only computed at sensor j for the total information contribution. Therefore, the information filter is computationally more efficient and more suitable for decentralized sensor estimation than the conventional Kalman filter.

3.2 Multiple Space Object Tracking

For the multiple space object tracking problem, the measurement-to-track association has to resolve which observation is assigned to which orbit. Figure 3 highlights that a gating region around a measurement is used to determine which measurements are valid before providing the measurement to the filter. In this paper, the GNN and JPDA algorithms are used to determine which measurements are associated with current tracks.

Before applying the GNN and JPDA algorithms, the gating procedure can be performed over the measurements in order to reduce the computational time, complexity, and the number of valid measurements. The typical ellipsoidal gate region is given as

$$[\mathbf{z}_k^m - \hat{\mathbf{z}}_{k|k-1}^l]^T \mathbf{M}^{-1} [\mathbf{z}_k^m - \hat{\mathbf{z}}_{k|k-1}^l] \leq \eta^2, \quad (25)$$

where \mathbf{M} is the covariance matrix corresponding to $\mathbf{z}_k^m - \hat{\mathbf{z}}_{k|k-1}^l$ and η is the threshold. Note that \mathbf{z}_k^m is the

m 'th measurement at time k and $\hat{\mathbf{z}}_{k|k-1}^l$ is the predicted measurement by the l 'th track.

To use the GNN algorithm, the distance is defined as $d_{ml} = [\mathbf{z}_k^m - \hat{\mathbf{z}}_{k|k-1}^l]^T \mathbf{M}^{-1} [\mathbf{z}_k^m - \hat{\mathbf{z}}_{k|k-1}^l]$. For each measurement from the sensor observation \mathbf{z}_k^m , the goal of the GNN algorithm is to choose assignments to minimize the distance. When a single measurement is gated to a single track, it is easy to associate the measurement and the track. For closely spaced targets, it is very likely that multiple measurements fall in a single gate. Simply assigning observations to tracks using minimization of distance could give a wrong assignment solution.²² Hence, the validated matrix \mathbf{D} should be constructed and used. The validated matrix with n measurements and p tracks is shown as

$$\mathbf{D} = \begin{bmatrix} d_{11} & d_{12} & d_{13} & \cdots & d_{1p} \\ d_{21} & d_{22} & d_{23} & \cdots & d_{2p} \\ \vdots & \vdots & \vdots & \ddots & \vdots \\ d_{n1} & d_{n2} & d_{n3} & \cdots & d_{np} \end{bmatrix}. \quad (26)$$

Recall that, for d_{ml} , “ m ” is used to denote the m 'th measurement and “ l ” denotes the track. The goal of the GNN is to find the assignment solution which minimizes the summed total distance using the validated matrix. In this paper, the Munkres algorithm²³ is used to find the measurement to track association pairs based on the validation matrix.

Remark 3.2: When the association pair is determined, the information state contribution $\mathbf{i}_{k,j}$ and the information matrix contribution $\mathbf{I}_{k,j}$ of the j 'th sensor can be obtained by Eqs. (19) and (20), respectively.

Similarly, the probabilistic data association algorithm can be used by each sensor to solve the measurement-to-track association problem. For convenience, $DA^{m,l}$ is used to denote the event that the l 'th space object track is associated with the m 'th measurement. Under this specific association, the innovation $\tilde{\mathbf{z}}_k^{m,l}$ and innovation covariance \mathbf{S}_k^l are given as

$$\tilde{\mathbf{z}}_k^{m,l} = \mathbf{z}_k^m - \mathbf{h}^l(\hat{\mathbf{x}}_{k|k-1}^l), \quad (27)$$

$$\mathbf{S}_k^l = (\mathbf{P}_{k|k-1,xz}^l)^T (\mathbf{P}_{k|k-1}^l)^{-1} \mathbf{P}_{k|k-1,xz}^l + \mathbf{R}^l, \quad (28)$$

where \mathbf{z}_k^m is the m 'th measurement, the superscript “ l ” denotes the l 'th track. Assume the probability that the data association $DA^{m,l}$ is denoted as $\beta^{m,l}$ and the probability that there is no measurement corresponding to the l 'th space object is $\beta^{0,l}$. The update procedure using the JPDA filter (JPDAF) for the l 'th space object can be written as

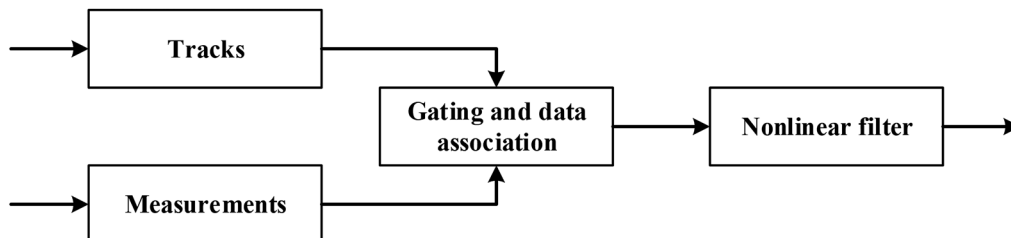


Fig. 3 The flowchart of the multiple space object tracking problem.

$$\hat{\mathbf{x}}_{k|k}^l = \hat{\mathbf{x}}_{k|k-1}^l + \mathbf{K}_k^l \tilde{\mathbf{v}}_k^l, \quad (29)$$

$$\mathbf{P}_{k|k}^l = \mathbf{P}_{k|k-1}^l - (1 - \beta^{0,l}) \mathbf{K}_k^l \mathbf{S}_k^l \mathbf{K}_k^{lT} + \mathbf{K}_k^l \tilde{\mathbf{P}}_k^l \mathbf{K}_k^{lT}, \quad (30)$$

where

$$\mathbf{K}_k^l = \mathbf{P}_{k|k-1, vz}^l (\mathbf{S}_k^l)^{-1}, \quad (31)$$

$$\tilde{\mathbf{v}}_k^l = \sum_{m=1}^M \beta^{m,l} \tilde{\mathbf{z}}_k^{m,l} = \mathbf{v}_k^l - (1 - \beta^{0,l}) \mathbf{h}^l(\hat{\mathbf{x}}_{k|k-1}^l), \quad (32)$$

$$\mathbf{v}_k^l = \sum_{m=1}^M \beta^{m,l} \mathbf{z}_k^m, \quad (33)$$

$$\tilde{\mathbf{P}}_k^l = \left[\sum_{m=1}^M \beta^{m,l} \tilde{\mathbf{z}}_k^{m,l} (\tilde{\mathbf{z}}_k^{m,l})^T \right] - \tilde{\mathbf{v}}_k^l (\tilde{\mathbf{v}}_k^l)^T, \quad (34)$$

and M is the number of validated measurements after gating. $\beta^{m,l}$ is given as

$$\beta^{m,l} = \begin{cases} \frac{\mathbf{L}^{m,l}}{1 - P_D P_G + \sum_{j=1}^M \mathbf{L}^{j,l}}, & m = 1, \dots, M \\ \frac{1 - P_D P_G}{1 - P_D P_G + \sum_{j=1}^M \mathbf{L}^{j,l}}, & m = 0 \end{cases}, \quad (35)$$

where P_D and P_G are the space object detection probability and gate probability, respectively. In addition,

$$\mathbf{L}^{m,l} = \frac{N(\mathbf{z}^m; \hat{\mathbf{z}}_{k|k-1}^l, \mathbf{S}_k^l) P_D}{\tilde{\lambda}}. \quad (36)$$

Note that $\hat{\mathbf{z}}_{k|k-1}^l$ is the predicted measurement. $\tilde{\lambda}$ is the density of the spatial Poisson process that models the clutter.

The information form of JPDA-based filtering algorithm has been derived.²⁴ Due to the association uncertainty, Eqs. (17) and (18) are revised. For convenience, we list these equations as follows:²⁴

$$\hat{\mathbf{x}}_{k|k}^l = \left(\mathbf{Y}_{k|k-1}^l + \sum_{j=1}^{N_{sn}} \mathbf{I}_{k,j}^l \right)^{-1} \left[\mathbf{Y}_{k|k-1}^l \hat{\mathbf{x}}_{k|k-1}^l + \sum_{j=1}^{N_{sn}} (\mathbf{i}_{k,j}^l + \beta_j^{0,l} \mathbf{I}_{k,j}^l \hat{\mathbf{x}}_{k|k-1,j}^l) \right], \quad (37)$$

$$\mathbf{Y}_{k|k}^l = \mathbf{Y}_{k|k-1}^l + \sum_{j=1}^{N_{sn}} \mathbf{G}_{k,j}^l, \quad (38)$$

where

$$\mathbf{G}_{k,j}^l = \mathbf{Y}_{k|k-1,j}^l \mathbf{K}_{k,j}^l \{ [(1 - \beta_j^{0,l}) \mathbf{S}_{k,j}^l - \tilde{\mathbf{P}}_{k,j}^l]^{-1} - (\mathbf{K}_{k,j}^l)^T \mathbf{Y}_{k|k-1,j}^l \mathbf{K}_{k,j}^l \}^{-1} (\mathbf{K}_{k,j}^l)^T \mathbf{Y}_{k|k-1,j}^l. \quad (39)$$

In summary, the information shared by each sensor includes \mathbf{I}_k^l , $\mathbf{i}_{k,j}^l + \beta_j^{0,l} \mathbf{I}_{k,j}^l \hat{\mathbf{x}}_{k|k-1,j}^l$, and $\mathbf{G}_{k,j}^l$.

4 Diffusion-Based Cooperative Space Object Tracking

The consensus strategy has been used to design the distributed space object tracking algorithm.^{4,25} One requirement to use the consensus strategy is sufficient communication between different sensors. However, communication resources are limited in space tracking applications. Hence, it is necessary to design a communication efficient, SpOT algorithm based on decentralized approaches. In this paper, the diffusion-based strategy is utilized for the decentralized SpOT. The diffusion strategy is typically used to solve linear distributed estimation problems. Although the linearization technique can be used to extend the diffusion strategy to solve the nonlinear estimation problem, the accuracy of the linearization is limited. Hence, the cubature rule is proposed to extend the traditional diffusion strategy. As shown in Fig. 4, there are two steps of the diffusion strategy-based distributed nonlinear filters, which are the incremental update and diffusion update. For the incremental update, at each time step, each agent will communicate with their neighbors the information state and information matrix to obtain an intermediate estimated result of the system state. The diffusion update is then conducted based on the

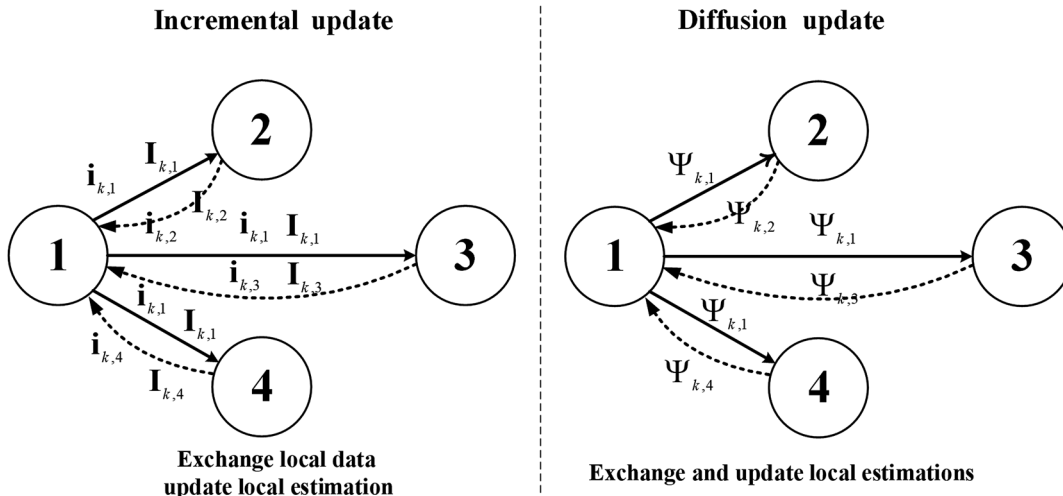


Fig. 4 Diffusion strategy based distributed nonlinear filter update at node 1.

intermediate estimate given by the incremental update step.⁷ Note that the symbol “ $\Psi_{k,i}$ ” with $i = 1, \dots, 4$ in Fig. 4 denotes the information shared by the i 'th sensor in the diffusion update step. The main reason to use the diffusion strategy for distributed space object tracking is that it only requires two information transmissions between different sensors. Hence, it can save communication resources in distributed and SpOT.

Rather than using the conventional diffusion strategy, we propose to use the enhanced diffusion strategy, which integrates 0-1 weighting covariance intersection and iterative covariance intersection (ICI) strategies. For convenience, the conventional diffusion strategy is described next with the proposed ICI strategy as follows.

4.1 Conventional Diffusion Strategy

The conventional diffusion strategy includes two steps: the incremental update and the diffusion update.⁷

4.1.1 Incremental update

In the incremental update step, each sensor will broadcast its information to neighbors. If the GNN algorithm is used, for every sensor j , after receiving the information from neighbors, the information state and covariance are obtained as

$$\hat{\mathbf{y}}_{k|k,j}^l = \hat{\mathbf{y}}_{k|k,j}^l + \sum_{j' \in N_j} \mathbf{i}_{k,j'}^l, \quad (40)$$

$$\mathbf{Y}_{k|k,j}^l = \mathbf{Y}_{k|k,j}^l + \sum_{j' \in N_j} \mathbf{I}_{k,j'}^l, \quad (41)$$

where N_j is the neighborhood set of sensor j , $\mathbf{i}_{k,j}$ is the information state contribution, and $\mathbf{I}_{k,j}$ is the information matrix contribution.

Note that if the JPDA algorithm is used, the state and the information covariance are obtained by Eqs. (37)–(39).

4.1.2 Diffusion update

In the diffusion update step, the intermediate state estimation can be updated as

$$\hat{\mathbf{x}}_{k,j}^l = \sum_{j' \in \tilde{N}_j} C_{j',j} \hat{\mathbf{x}}_{k,j'}^l. \quad (42)$$

Note that the weighting coefficients $C_{j',j}$ should satisfy the constraint $\sum_{j'=1}^{N_{sm}} c_{j',j} = 1$ where \tilde{N}_j is the neighborhood set of sensor j , including itself.

There are many ways to choose the weighting coefficients. In this paper, the covariance intersection algorithm is employed due to its simplicity to determine the weighting coefficients. Note that the covariance intersection algorithm does not consider the cross-correlation between different sensor estimations, which may slightly affect the estimation accuracy. However, in the SpOT applications, it provides satisfactory results. For convenience, we omit the superscript “ l ” and subscript “ k ” in the following discussion for each track.

The fused state can be obtained via the covariance intersection algorithm as²⁶

$$(\hat{\mathbf{P}}_j)^{-1} \hat{\mathbf{x}}_j = \sum_{j' \in \tilde{N}_j} \omega_{j',j} (\mathbf{P}_{j'})^{-1} \mathbf{x}_{j'}, \quad (43)$$

where the covariance $\hat{\mathbf{P}}_j$ is given as²⁶

$$(\hat{\mathbf{P}}_j)^{-1} = \sum_{j' \in \tilde{N}_j} \omega_{j',j} (\mathbf{P}_{j'})^{-1}. \quad (44)$$

Note that $\mathbf{x}_{j'}$ and $\mathbf{P}_{j'}$ are the state estimation given by the j' 'th sensor and the weights are

$$\omega_{j',j} = \frac{1/\text{tr}(\mathbf{P}_{j'})}{\sum_{j' \in \tilde{N}_j} 1/\text{tr}(\mathbf{P}_{j'})}, \quad (45)$$

where that “ $\text{tr}(\cdot)$ ” is the trace operator.

Using Eqs. (43)–(45), $\hat{\mathbf{x}}_{k,j}^l$ in Eq. (42) can be updated. Then, the state can be predicted according to Eqs. (11)–(16).

4.2 Enhanced Diffusion Strategy

The proposed enhanced diffusion strategy using covariance intersection includes two steps: the incremental update and the diffusion update. The incremental update is the same as in the conventional diffusion strategy, but the diffusion update is revised with the consideration of naïve sensors (without measurement) and communications resources. Due to the variation of the geometric relations between sensors, the Sun, the Earth, and the space object; there are some sensors without any measurements. For the sensors without measurements, the estimation is predicted from the previous state estimation. Due to the lack of observations, the estimation accuracy of these sensors can be very low. When there are no measurements of low-accuracy measurements, the traditional diffusion strategy using the covariance intersection may degrade or fail. To overcome this problem, rather than use Eqs. (43)–(45) to calculate the weight, a 0-1 weighting strategy is utilized. For the j' 'th sensor, the weight can be calculated as

$$\omega_{j',j} = \begin{cases} 1 & \text{if } j' = m_{j',j} \\ 0 & \text{otherwise} \end{cases}, \quad (46)$$

where $m_{j',j} = \min_{j' \in \tilde{N}_j} \text{tr}(\mathbf{P}_{j'})$.

The 0-1 weighting strategy can overcome or mitigate the problem of lacking observations for some sensors. For the 0-1 weighting strategy, the fusion result is the estimation of the sensor with minimum uncertainty. Note that the trace of the covariance matrix is used to measure the uncertainty of the estimation. Specifically, the trace of the covariance matrix denotes the overall expected mean squared error.²⁷

In general, the sensor estimation with observation gives better estimation result than the sensor estimation without measurement. By using 0-1 weighting strategy, only the best estimation is preserved. The information of other sensors is discarded. Hence, the effect of the sensor without observations is overcome or mitigated.

For the covariance intersection, the drawback of the 0-1 weighting strategy is that only the state estimation with minimal trace of the covariance is used and the information from other sensors in the diffusion update step will not be used. To improve the performance, the conventional weighting is

combined with the 0-1 weighting to calculate the final estimate. For convenience, we denote:

Strategy 1: the state and covariance given by the conventional weighting strategy are denoted by $\hat{\mathbf{x}}_j^{(1)}$ and $\hat{\mathbf{P}}_j^{(1)}$,

Strategy 2: the state and covariance given by the 0-1 weighting strategy are denoted by $\hat{\mathbf{x}}_j^{(2)}$ and $\hat{\mathbf{P}}_j^{(2)}$.

The proposed diffusion strategy enhances the covariance intersection strategy by integrating these two strategies. The fused state $\hat{\mathbf{x}}_{j,f}$ and covariance $\hat{\mathbf{P}}_{j,f}$ are given as

$$(\hat{\mathbf{x}}_{j,f}, \hat{\mathbf{P}}_{j,f}) = \begin{cases} [\hat{\mathbf{x}}_j^{(1)}, \hat{\mathbf{P}}_j^{(1)}] & \text{if } \text{tr}[\hat{\mathbf{P}}_j^{(1)}] \leq \text{tr}[\hat{\mathbf{P}}_j^{(2)}] \\ [\hat{\mathbf{x}}_j^{(2)}, \hat{\mathbf{P}}_j^{(2)}] & \text{otherwise} \end{cases}. \quad (47)$$

According to Eq. (47), the final estimation is the better one between the estimation given by strategy 1 and strategy 2. The strategy 2 overcomes or mitigates the effect of the lack of observations. If strategy 1 is strongly affected by the lack of observations problem, the performance of strategy 1 will degrade. In this case, strategy 2 will be used. Hence, Eq. (47) can also overcome or mitigate the lack of observations problem.

In addition, we propose to use the ICI in the diffusion step. For convenience, we name the proposed filter as the diffusion-based filter (D) with the enhanced iterative covariance intersection (EICI) strategy (D-EICI). A typical cycle of D-EICI is summarized in Fig. 5. After the incremental update, the enhanced covariance intersection solution for

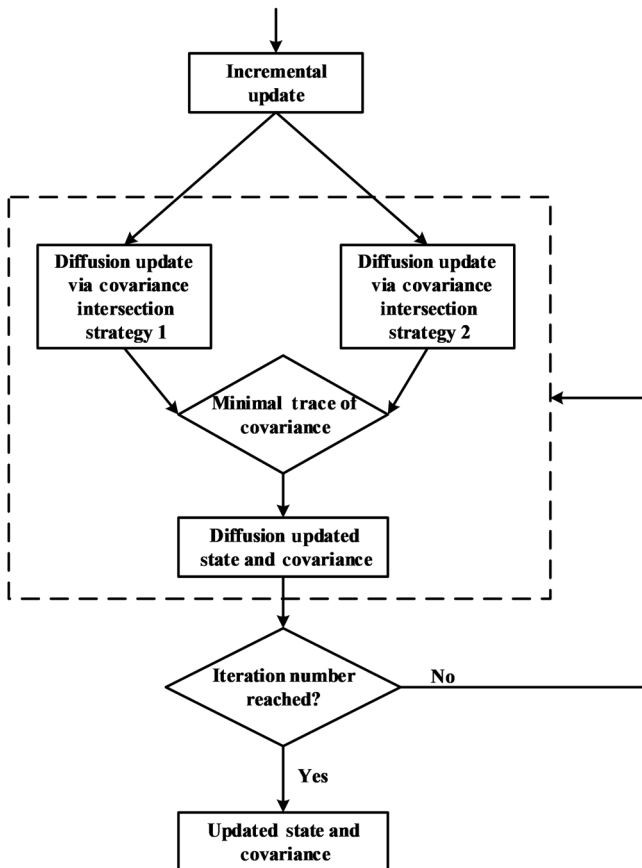


Fig. 5 The flowchart of the diffusion-based EICI filter.

the diffusion update is determined. The diffusion update result is determined by either the conventional covariance intersection or covariance intersection with 0-1 weighting strategy, according to Eq. (47). In addition, multiple iterations can be used in the diffusion step. The performance is improved by repeating the enhanced covariance intersection strategy multiple times. The improvement is a result that information exchange is more sufficient by using multiple time information exchanges between neighbors for distributed estimation.

5 Numerical Experiments

In order to test the performance of the proposed diffusion-based enhanced iterative covariance intersection (D-EICI) filter for space object tracking (DeCiSpOT), two scenarios are provided. One is for cooperative single space object tracking and the second is for cooperative multiple space object tracking. In both scenarios, 10 ground EO sensors are used. Locations of these sensors are shown in Table 1. Note that the location is represented by latitude and longitude.

Table 1 EO sensor locations.

Sensor index	Location
1	42.62°N, 71.49°W
2	52.7°N 174.1°E
3	30.57°N 86.22°E
4	70.37°N 31.13°E
5	32.82°N 106.66°W
6	7.41°S 72.45°E
7	20.71°N 156.26°W
8	8.71°N 167.73°E
9	37.17°N 5.62°W

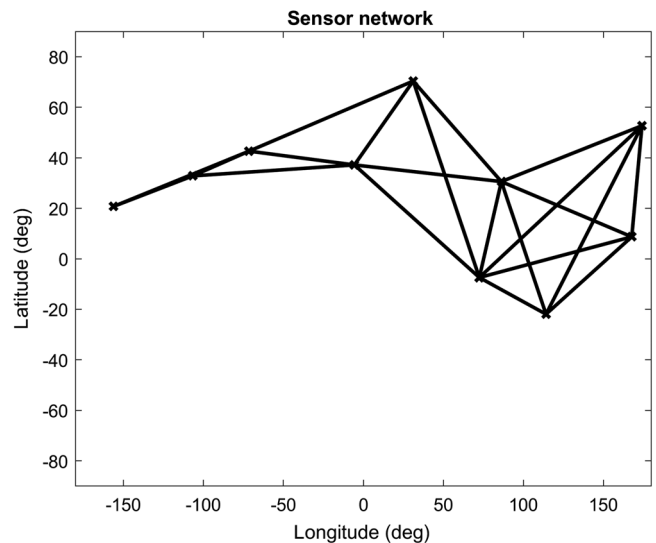


Fig. 6 Topology of the EO space object sensing network.

These sensors cooperatively track Geosynchronous Earth Orbit (GEO) objects. For the distributed SpOT, the topology of the network should be given. In the simulation, the topology of the network is shown in Fig. 6. Note that the symbol “x” denotes the sensor and the solid line denotes the link between different sensors.

5.1 Single GEO Object Tracking

A GEO object is used and the initial state of the object is $\mathbf{x}_0 = [(\mathbf{x}_{0, \text{pos}})^T, (\mathbf{x}_{0, \text{vel}})^T]^T$, where $\mathbf{x}_{0, \text{pos}} = [42261.2813 \text{ km}, 4882.9648 \text{ km}, 1344.2211 \text{ km}]^T$ and $\mathbf{x}_{0, \text{vel}} = [-0.3682 \text{ km/s}, 2.9286 \text{ km/s}, 0.8005 \text{ km/s}]^T$. The initial covariance is given by $\mathbf{P}_0 = \text{diag}([100 \text{ km}^2, 100 \text{ km}^2, 100 \text{ km}^2, 0.01 \text{ km}^2/\text{s}^2, 0.01 \text{ km}^2/\text{s}^2, 0.01 \text{ km}^2/\text{s}^2])$. The adaptive step size Runge–Kutta method is used to propagate the orbit [Eq. (1)] and the measurement period is 60 s. Five different filters, including (1) the centralized cubature Kalman filter, (2) the diffusion-based filter with enhanced covariance intersection strategy (D-EICI), which is based on the integration of strategy 1 and strategy 2, (3) the D-EICI, (4) the diffusion-based filter with covariance intersection filter using plain 0-1 weighting strategy (D-CI), and (5) the diffusion-based filter with ICI using plain 0-1 weighting strategy (D-ICI), are tested.

Fifty Monte Carlo runs are conducted, and the root mean square error (RMSE) for the position and velocity are shown in Figs. 7 and 8, respectively. Note that the results from the traditional diffusion-based filters are not shown since they do not consider the naïve node. In addition, due to the paper limitations, only the result from the first sensor is shown and the results of other sensors follow the same trend. From Figs. 7 and 8, it can be seen that the performance of all diffusion-based filters is improved by increasing the number of information exchanges. Note that “N” is used to denote the number of information exchanges in Figs. 7 and 8. Specifically, the performance of all diffusion-based filters with 10 diffusion update iterations have better performance than filters with a single diffusion update. However, the information exchange in the network converges to a sufficient value with the increasing of the number of information exchanges.

In addition, the D-EICI has better performance than the D-ICI, which demonstrates the effectiveness of the proposed

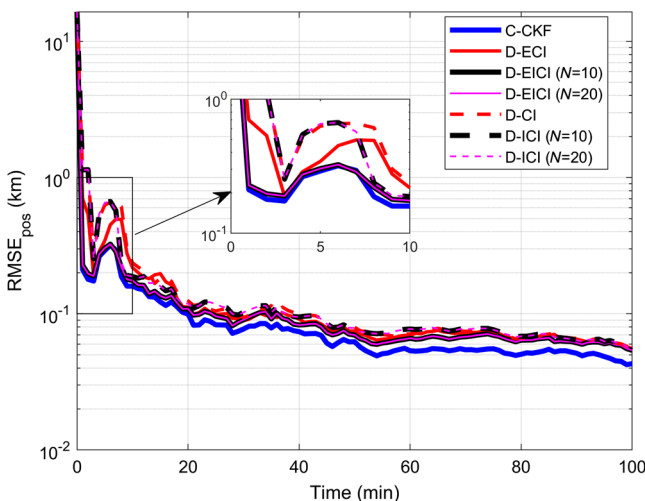


Fig. 7 RMSE position error for the centralized and diffusion filters.

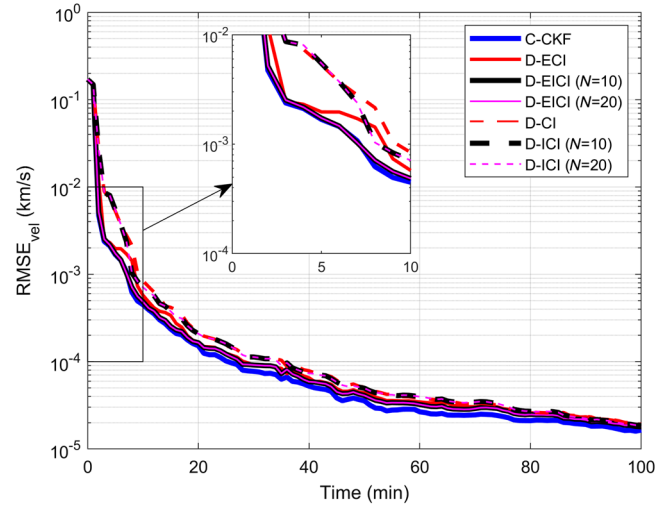


Fig. 8 RMSE velocity error for the centralized and diffusion filters.

EICI strategy. One thing to emphasize is that the proposed D-EICI is flexible in terms of communication resources. When the communication resources are sufficient, the number of information exchanges can be large. When the communication resources are limited, only two information exchanges are required for a satisfactory performance.

5.2 Multiple GEO Object Tracking

To evaluate the performance of the multiple space object tracking using the proposed diffusion algorithms in Sec. 4, five space objects are used. The trajectories of the five space objects are shown in Fig. 9 and their initial states are given in Table 2. The initial covariance is the same as \mathbf{P}_0 in scenario 1. The observations and tracks are associated by the GNN or JPDA algorithm described in Sec. 4. Each sensor updates the state of multiple space objects and shared the information with neighbors by the enhanced diffusion strategy. Note that in the simulation, $p_G = 0.99$, which means 99% validation region is used for the measurement and the gating threshold is $\eta = 9.2$. The clutter is generated uniformly with the number of clutter points, which are obtained from a Poisson distribution with spatial density $10^{-9}/\text{km}^3$ in a cuboid. The center of the cuboid is assumed to be the

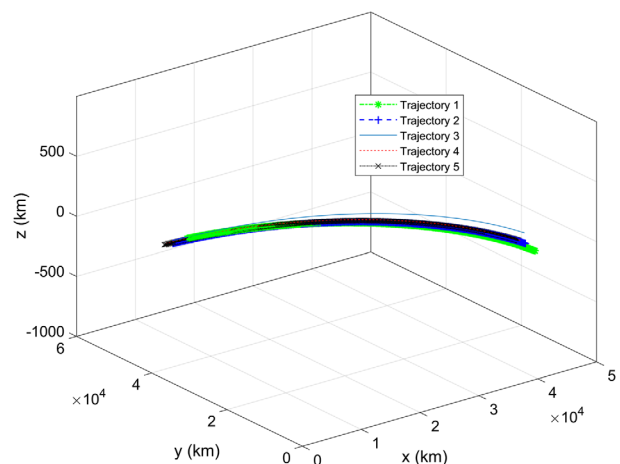


Fig. 9 The trajectories of the five space objects.

Table 2 Initial states of the five space objects.

Space object index	Initial state
1	$\mathbf{x}_0 = [41995.87 \text{ km}, 3836.69 \text{ km}, -21.42 \text{ km}, -0.2802 \text{ km/s}, 3.0614 \text{ km/s}, 0.00032 \text{ km/s}]^T$
2	$\mathbf{x}_0 = [41731.13 \text{ km}, 6029.50 \text{ km}, 10.28 \text{ km}, -0.4398 \text{ km/s}, 3.0431 \text{ km/s}, -0.0016 \text{ km/s}]^T$
3	$\mathbf{x}_0 = [41730.10 \text{ km}, 6223.09 \text{ km}, 94.97 \text{ km}, -0.4529 \text{ km/s}, 3.0391 \text{ km/s}, -0.0017 \text{ km/s}]^T$
4	$\mathbf{x}_0 = [41564.13 \text{ km}, 7115.81 \text{ km}, 22.22 \text{ km}, -0.5189 \text{ km/s}, 3.0303 \text{ km/s}, -0.0006 \text{ km/s}]^T$
5	$\mathbf{x}_0 = [41518.91 \text{ km}, 7392.15 \text{ km}, 17.52 \text{ km}, -0.5393 \text{ km/s}, 3.0265 \text{ km/s}, -0.0012 \text{ km/s}]^T$

average value of positions of all five space objects. The dimension size of the cuboid is given by 500 km × 500 km × 100 km. Note that “500 km” corresponds to the in-track and cross-track direction and “100 km” corresponds to the radial direction. The detection probability is assumed to be $p_D = 0.995$.

Due to the variation of the geometry between the Sun, the Earth, space objects, and sensors; the number of valid sensor measurements for different space objects varies, as can be seen from Fig. 10. In some cases, multiple sensors could observe the same space object. Note that spikes in Fig. 10 are caused by imperfect detection of the measurement. Similarly, the number of observation changes with time for different sensors, as can be seen from Fig. 11. Note that the upper spikes are caused by the clutter and the lower spikes are caused by imperfect measurement detections.

Different filters, including the centralized and D-EICI filter and corresponding iterative version (D-EICI) filter with GNN and JPDA algorithms, are tested, which extend methods in consensus-based space object tracking. The optimal subpattern assignment (OSPA)²⁸ distance is used to measure the quality of estimation. Fifty Monte Carlo runs are conducted and the average OSPA distance is shown in Fig. 12. It can be seen that the centralized CKF with the JPDA algorithm has the best performance but the proposed filter, the D-EICI, achieves performance close to the centralized method.

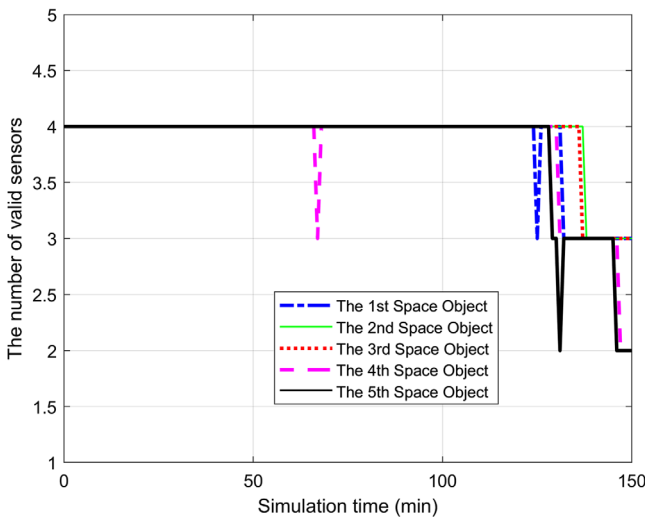


Fig. 10 The number of valid sensors for different space objects (1 to 5).

In addition, it can be seen that the D-EICI with multiple information exchanges (10 times) has better performance than the D-EICI without multiple information exchanges. Note that for both D-EICI and D-EICI, the JPDA strategy is used. Filters using the JPDA strategy have better performance than those using the GNN strategy. In addition, the

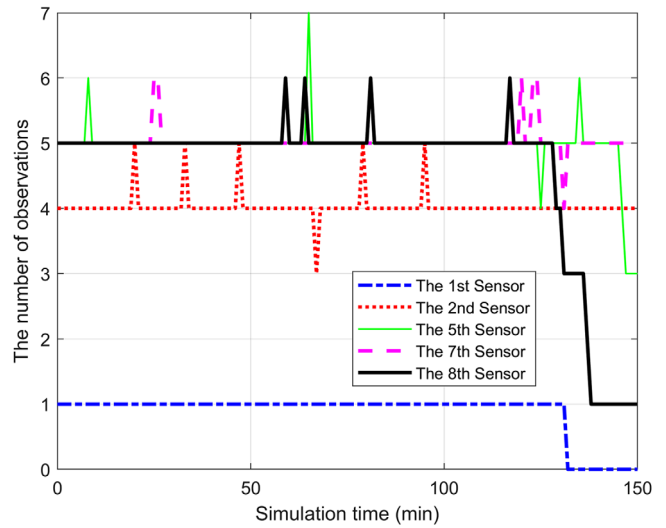


Fig. 11 The number of observations for different sensors (1 to 10).

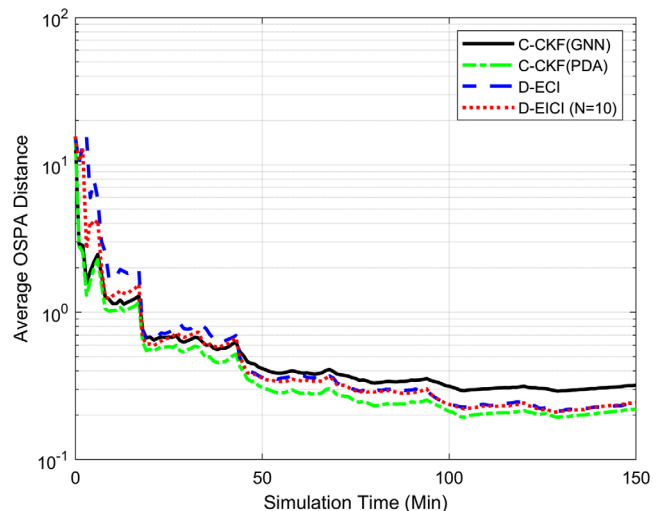


Fig. 12 The average OSPA distance.

centralized GNN-based filter has worse performance than the filter using the JPDA strategy for this scenario.

Note that, it is possible to use the proposed algorithm with variants of JPDA and GNN for different space object tracking scenarios. The performance of the filter, however, is problem dependent.

6 Conclusion

The D-EICI cooperative space object tracking (DeCiSpOT) filter is proposed for distributed multiple sensor SpOT. Two space object tracking scenarios are used to demonstrate the effectiveness of the proposed DeCiSpOT to support SSA. The paper demonstrates that satisfactory performance can be achieved with the DeCiSpOT filter which balances the communication resources and computational complexity, especially in cases where measurements are obscured and/or of low accuracy. When the communication resources are limited, only two information exchanges are required for sufficient performance. When the communication resources are available, a large number of information exchanges can be used with the information filter method. For the multiple space object tracking problem, the diffusion-based nonlinear filtering framework accommodates the JPDA and GNN algorithms used within. The diffusion-based approaches show promising performance in single and multiple space object tracking problems, which provides a solution for time-sensitive space object tracking tasks.

Future work would include the use of space object recognition for measurement selection using the joint-belief probabilistic data association filter,²⁹ multimodal information from ground-based radar and EO sensors,³⁰ as well as multidomain coordination between ground and space sensors.³¹

Acknowledgments

This research was partly supported by the Air Force Research Laboratory under contract number FA9453-15-C-0459. The views and conclusions contained herein are those of the authors and should not be interpreted as necessarily representing the official policies or endorsements, either expressed or implied, of the United States Air Force.

References

1. W. Brian, P. Cefola, and J. Sankaran, "Global space situational awareness sensors," in *AMOS Conf.* (2010).
2. K. Demars et al., "Multiple-object space surveillance tracking using finite-set statistics," *AIAA J. Guidance Control Dyn.* **38**(9), 1741–1756 (2015).
3. B. Jia et al., "Multiple space object tracking via a space-based optical sensor," in *IEEE Aerospace Conf.* (2016).
4. B. Jia et al., "Cooperative space object tracking using consensus-based filters," in *17th Int. Conf. Information Fusion* (2014).
5. S. Kar and J. Moura, "Gossip and distributed Kalman filtering: weak consensus under weak detectability," *IEEE Trans. Signal Process.* **59**(4), 1766–1784 (2011).
6. R. Olfati-Saber, J. A. Fax, and R. M. Murray, "Consensus and cooperation in networked multi-agent systems," *Proc. IEEE* **95**(1), 215–233 (2007).
7. F. S. Cattivelli and A. H. Sayed, "Diffusion strategies for distributed Kalman filtering and smoothing," *IEEE Trans. Autom. Control* **55**(9), 2069–2084 (2010).
8. A. T. Kamal, J. A. Farrell, and A. K. Roy-Chowdhury, "Information weighted consensus," in *IEEE Conf. Decision and Control* (2012).
9. J. T. Horwood, N. D. Aragon, and A. B. Poore, "Covariance consistency for track initiation using Gauss–Hermite quadrature," *Proc. SPIE* **7698**, 76980T (2010).
10. B. Sease et al., "Enabling direct feedback between initial orbit determination and sensor data processing for detection and tracking of space objects," *Proc. SPIE* **9469**, 94690M (2015).

11. Y. Bar-Shalom, *Multitarget/Multisensor Tracking: Applications and Advances*, Artech House Radar Library, Norwood, Massachusetts (2000).
12. S. J. Julier and J. K. Uhlmann, "Unscented filtering and nonlinear estimation," *Proc. IEEE* **92**(3), 401–422 (2004).
13. I. Arasaratnam and S. Haykin, "Cubature Kalman filters," *IEEE Trans. Autom. Control* **54**(6), 1254–1269 (2009).
14. B. Jia, M. Xin, and Y. Cheng, "High-degree cubature Kalman filter," *Automatica* **49**(2), 510–518 (2013).
15. B. Jia, M. Xin, and Y. Cheng, "Sparse Gauss–Hermite quadrature filter with application to spacecraft attitude estimation," *J. Guidance Control Dyn.* **34**(2), 367–379 (2011).
16. B. Jia, M. Xin, and Y. Cheng, "Sparse-grid quadrature nonlinear filtering," *Automatica* **48**(2), 327–341 (2012).
17. G. Seeber, *Satellite Geodesy*, 2nd ed., Walter de Gruyter, New York (2003).
18. B. O. S. Teixeira et al., "Spacecraft tracking using sampled-data Kalman filters," *IEEE Control Syst. Mag.* **28**(4), 78–94 (2008).
19. A. T. Hobson, "Sensor management for enhanced catalogue maintenance of resident space objects," PhD thesis, The University of Queensland (2014).
20. B. Jia and M. Xin, "Multiple sensor estimation using a new fifth-degree cubature information filter," *Trans. Inst. Meas. Control* **37**(1), 15–24 (2015).
21. D. Lee, "Nonlinear estimation and multiple sensor fusion using unscented information filtering," *IEEE Signal Process. Lett.* **15**, 861–864 (2008).
22. P. Konstantinova, A. Udvarov, and T. Semerdjiev, "A study of a target tracking algorithm using global nearest neighbor approach," in *Proc. 4th Int. Conf. Computer Systems and Technologies: e-Learning*, pp. 290–295 (2003).
23. F. Bourgeois and J. Lassalle, "An extension of the Munkres algorithm for the assignment problem to rectangular matrices," *Commun. ACM* **14**(12), 802–804 (1971).
24. A. T. Kamal, J. A. Farrell, and A. K. Roy-Chowdhury, "Information consensus for distributed multi-target tracking," in *IEEE Conf. Computer Vision and Pattern Recognition*, pp. 2403–2410 (2013).
25. B. Jia et al., "Cooperative space object tracking using space-based optical sensors via consensus-based filters," *IEEE Trans. Aerosp. Electron. Syst.* **52**(4), 1908–1936 (2016).
26. W. Niehsen, "Information fusion based on fast covariance intersection filtering," in *Proc. Fifth Int. Conf. Information Fusion*, Annapolis, Maryland, pp. 901–904 (2002).
27. C. Yang, L. Kaplan, and E. Blasch, "Performance measures of covariance and information matrices in resource management for target state estimation," *IEEE Trans. Aerosp. Electron. Syst.* **48**(3), 2594–2613 (2012).
28. D. Schuhmacher, B. T. Vo, and B. N. A. Vo, "Consistent metric for performance evaluation of multiobject filters," *IEEE Trans. Signal Process.* **56**(8), 3447–3457 (2008).
29. E. Blasch, "Derivation of a belief filter for simultaneous high range resolution radar tracking and identification," PhD Thesis, Wright State University (1999).
30. A. Zatezalo et al., "Optimal constellation design of low earth orbit (LEO) EO/IR sensor platforms for space situational awareness," *Proc. SPIE* **7330**, 73300T (2009).
31. L. M. Simms et al., "Space-based telescopes for actionable refinement of ephemeris pathfinder mission," *Opt. Eng.* **51**(1), 011004 (2012).

Bin Jia received his PhD in the Department of Aerospace Engineering from Mississippi State University, Starkville, Mississippi, USA, in 2012. He works at Intelligent Fusion Technology, Inc., Germantown, Maryland, USA, as a project manager. His research interests include optimization, statistical signal processing, nonlinear filtering and estimation, guidance and navigation, and sensor fusion. Prior to IFT, he worked as a post-doctoral research scientist with the Department of Electrical Engineering, Columbia University, New York, New York, USA.

Khanh Pham serves as a senior aerospace engineer with the Air Force Research Laboratory-Space Vehicles Directorate. He is a senior member of IEEE, SPIE, and an associate fellow of AIAA. He received his BS and MS degrees in electrical engineering from the University of Nebraska and his PhD in electrical engineering from the University of Notre Dame. His research interests include statistical optimal control and estimation, dynamic game decision optimization, security of cyber-physical systems, and satellite cognitive radios.

Erik Blasch received his BS degree in mechanical engineering from Massachusetts Institute of Technology in 1992 and his PhD in electrical engineering from Wright State University in 1999. He has been with the Air Force Research Laboratory since 1996 compiling over

500 papers. He is a fellow of IEEE, fellow of SPIE, and associate fellow of AIAA. His areas of research include target tracking, image fusion, information fusion performance evaluation, and human-machine integration.

Genshe Chen received his BS and MS degrees in electrical engineering, PhD in aerospace engineering, in 1989, 1991, and 1994 respectively, all from Northwestern Polytechnical University, Xian, China. Currently, he is the chief technology officer of Intelligent Fusion Technologies, Inc., Germantown, Maryland, USA. His research interests include cooperative control and optimization for military operations, target tracking and multisensor fusion C4ISR, electronic

digital signal processing and image processing, game theoretic estimation and control.

Dan Shen received his BS degree in automation from Tsinghua University in 1998 and his MS and PhD degrees in electrical engineering from Ohio State University in 2003 and 2006, respectively. He is currently a principal scientist of the Intelligent Fusion Technology, Inc., Germantown, Maryland, USA. His research interest include information fusion, data mining, signal processing, dynamic game theory and applications, cooperative control and decision making, cyber network security, and space communication systems.